Research and Full Length Article:

Estimating Plant Dry Matter Productivity for AL-Sweeda Badia Rangeland (Syria) at Different Processing Levels of BKA, KVA Satellite Images

Ghadir Hmeidan [A]*, Ahed Alboody[B]

[A] Receiving and Processing Department, Space Technology Center, General Organization of Remote Sensing GORS, Damascus, Syria *(Corresponding author), Email: ghadir.hmeidan@yahoo.com

[B] Head of Integration & Testing and Maintenance Department, Space Technology Center, General Organization of Remote Sensing GORS, Damascus, Syria

Abstract. Estimation of plant dry matter to management of rangelands with high accuracy is important for managers. This research aims to compare Plant Dry Matter Productivity (PDMP) values estimated by Normalized Difference Vegetation Index (NDVI) derived from satellite images of BKA and KVA according to different levels of satellite image processing for AL-Sweeda Badia (Syria) during April and July in 2015 and October 2014. NDVI was calculated according to Digital Number values (DN); then, Top of Atmosphere values (TOA), and Ground Surface (GS) values after Atmospheric Correction (AC) were computed from L8 satellite images simultaneously with field measurements. A relationship between two time-dependent satellite images was created. Then, the derived relationships were adopted by L8 (PDMP) relationship estimation. Matter productivity average values according to TOA and GS were 15-42, 969-214, 3254-22 and 576-563 kg/h for the previous dates, respectively. There was a weak non-significant correlation between DN values and Matter productivity (≤0.063). And for TOA level, the relationship was relatively weak but significant (≤0.5). After atmospheric correction, it was strong (≥0.7) and significant at 1% and 5% levels and field verification measurements were consistent with 2014. A relationship between NDVI and PDMP for each previous value was determined according to NDVI values of modern images. Previous relationships were applied to estimate PDMP; then, objective maps were produced. DN satellite images as well as TOA values but at lower rate contained geometrical distortions resulting from terrain, climate, velocity changes, and sensor height and radiation refraction in atmosphere. Using GS after AC was good in rangelands for predicting and estimating PDMP.

Introduction

Syrian rangelands suffer from degradation factors such as overgrazing and agriculture. Remote sensing technologies are used to control rangelands for protecting them from degradation (Tanser and Palmer, 1999). Nordblom *et al.* (1997) estimated Syrian rangeland productivity of dry matter at 200 kg/h/year. Roland and Ilaiwib (2004) adopted digital number values (DN) for LandSat7 (L7) and NOAA images to study vegetation cover of Al-Bishri Mountain in Syria during 1981 and 1996. Ronald (2005) calibrated radiometer DN and satellite image DN to study vegetation cover and plant species in the Syrian Desert Rangeland. A comprehensive database was built for Syrian Rangeland (ACSAD, 2004) with a simple visual interpretation of three L5.7 images (1993, 2001 and 2002). Deep and Idris (2006) proposed a model for the estimation of rangeland capacity using ASTER satellite images (15m). Comparisons between different sensors have been made in several studies to ensure continuity and timeliness of data (updating the time series of images from different satellites) to control and model natural resources (Hanqiu and Zhang, 2011; Yin *et al.*, 2012). Miura *et al.* (2008) used two sensor images, low spatial resolution MODIS (250 to 500m) and Medium resolution ASTER (15m) with ground-level values (GS) after atmospheric error correction; after vegetation index was calculated (NDVI, EVI, EVI2), they found that $ASTER_{NDVI}$ was higher than $MODIS_{NDVI}$ while it was opposite for other indices. Researchers found that to obtain accuracy in results when using more than one type of images, calibration of each simultaneous image must be done because of a relationship between image changes from month to another plus deferent images resolution. Abuzar *et al.* (2014) suggested that various spatial images should be calibrated on Landsat satellite images.

There was a study of areas planted with fruit trees in northeastern Australia using several types of images L7 (30 m), ASTER, SPOT-5 XS (10 m) and RapidEye (5 m), QuickBird-2 (2.4 m), and WorldView-2 (2 m). Differences were significant (0.001) between ASTER, SPOT-5, RapidEye and non-significant between QuickBird-2 and WorldView-2. Théau *et al.* (2010) used satellite images of L5-TM (28.5m), SPOT-5HRG (10m), QuickBird-2 (2.5m) and MODIS (250m) and found that there was no effect of the space taken in one image to reduce spatial accuracy by assembling number of pixels, and it was worse for completing time series by different spatial resolution images. Whereas Liqin *et al.* (2014) calculated number of vegetation index from L7 and ASTER according to Top of Atmosphere Values (TOA) without calibrating or comparing two types of images. Thenkabail (2004) found a linking model between satellite images values taken by IKONOS and L7, where $IKONOS_{NDVI}$ was highly correlated with $L7_{NDVI}$ (0.67 to 0.72). Hanqiu and Zhang (2011) obtained a model to convert NDVI data between two satellite images also from ASTER and L7. Results showed that there were differences between NDVI data despite of a very strong positive linear relationship between them and ASTER sensors generally produced lower NDVI values than L7. According to Soudani *et al.* (2006), conversion factors were created between satellite images of different satellites of L7, SPOT HRV and IKONOS. Each sensor has its own characteristics such as high orbit, Special Resolution, Spectral Resolutions, Wavelength Band Limits, and Relative Spectral Response of Sensor. So, it is important to analyze interactions and quantitative relationships between multiple dependencies of image products to standardize quantitative standards and obtain good results (Liqin *et al.*, 2014).

Materials and Methods

This paper studied possibility of applying and using modern satellite images (not previously used in Syria) during 2014 and 2015 from Russian satellite Kanopus-V and Belarusian one Belka with spatial resolution 10.5 m (Nekrasova and Makushevaa, 2012; Eremeev *et al.*, 2014) and L7 and L8 satellites with spatial resolution 30 m compatible with previous images to study each of following:

1-Comparing NDVI between multiple spatial resolution images used in the research and finding a correlation between $L8_{NDVI}$, BKA_{NDVI} (Belka satellite) and KVA_{NDVI} (Kanopus V satellite)

2-Studying NDVI changes and estimating plant dry matter productivity in study area of al-Sweeda Badiya (Syria) using BKA and KVA satellite images compatible with L8 satellite images, whose plant dry matter productivity was previously estimated (Hmeidan *et al.*, 2016).

Materials
1-Location of study area

It is located within the al-Sweeda Badiya rangeland in south of Syria on Syrian-Jordanian border and includes total area of 16 thousand hectares (ACSAD, 2004).

2-Field Measurements

Field measurements were taken between 18 and 21/05/2004 and 03-04-05/2014 (some of the sites available within ACCSAD database (2004) dated compatible with date of satellite image L7 (25/5/2004) by Owensby (1973) method, modified in ACCSAD (Diop, 1998; fwal *et al.*, 2009; Al-Khalif *et al.*, 2009).

3-Satellite Images

L8 satellite images with medium spatial resolution 30 m (15 m Panchromatic, 16 temporary resolution, 16 bit, total coverage 185 km^2) and KVA, and BKA images with high spatial resolution 10.5 m (2.1 m Panchromatic,16 temporary resolution or by order, 11 bit, total coverage by order (ex 600×20=12000 km^2) (ground station of receiving satellite data in General organization of Remote Sensing) were used (Nekrasova and Makushevaa, 2012; Eremeev *et al.*, 2014) with dates shown in Table 1.

Table 1. Satellite images

Time	Date	Cycle	Sensor	Time	Date	Row	Path	Sensor
11:57:51	2014/10/09	12290	BKA	08:04:42	2014/10/04	37	173	L8
12:04:41	2015/04/18	15195	KVA	08:03:54	2015/04/14	37	173	L8
11:50:05	2015/04/23	15271	KVA	08:03:46	2015/04/30	37	173	L8
11:56:23	2015/07/30	16754	BKA	08:04:08	2015/08/04	37	173	L8

4-Research Outline

Fig. 1 shows research outline and production steps of maps to estimate dry weight plant productivity from L7 and L8 satellite images of study area, and relationships of $L8_{NDVI}$, BKA_{NDVI} and KVA_{NDVI} images to produce objective maps.
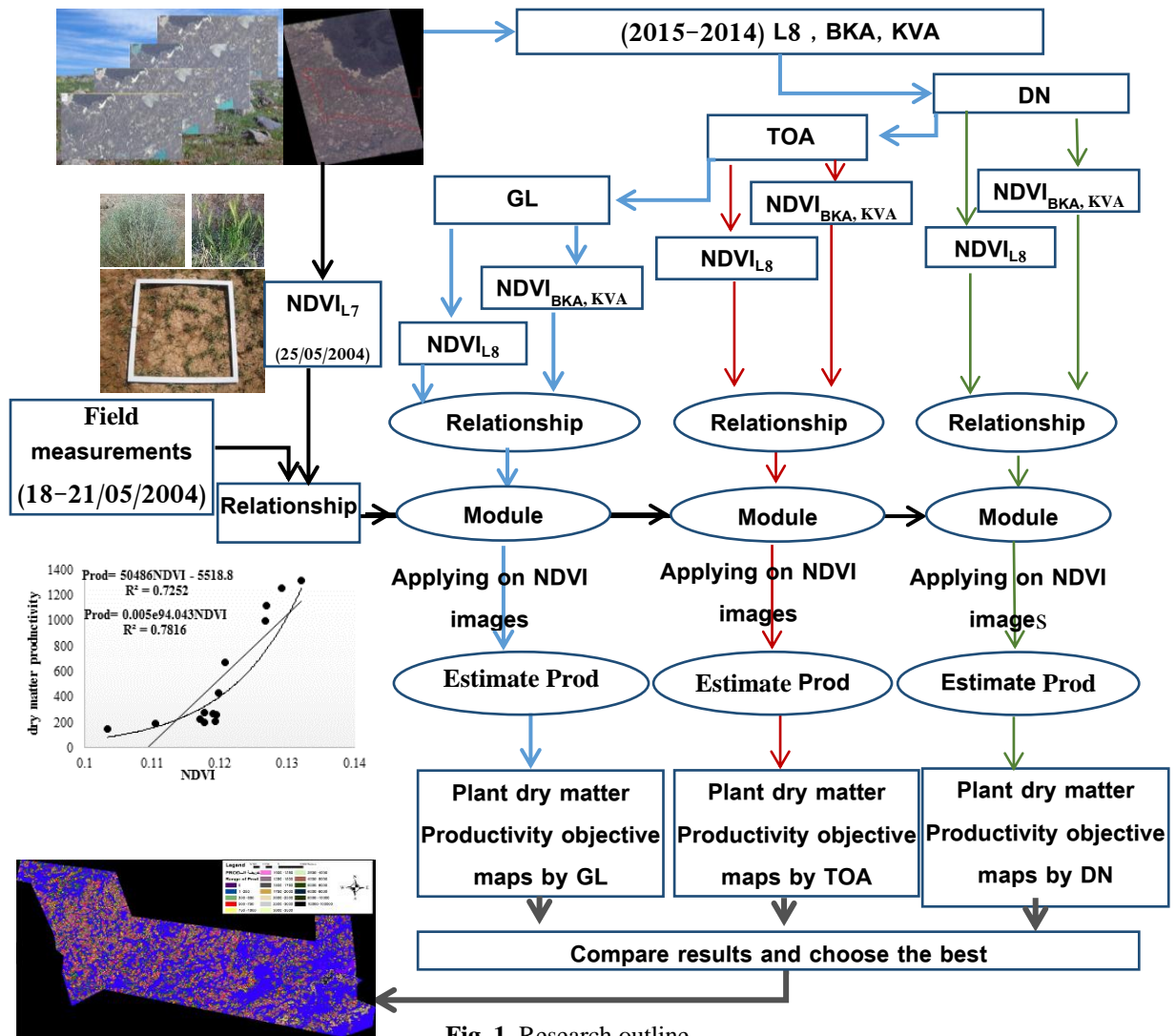
Fig. 1. Research outline

Methods

1-Satellite images processing and NDVI calculation

Analysis and preprocessing for satellite images were done through DN conversion into RAD values, TOA and finally, GS with the aim of calculating NDVI. (Felde *et al.,* 2003; Chander and Markham, 2003; Chander *et al.,* 2009; Parente, 2013; Mishra *et al.,* 2014):

$$L_\lambda = \left\{ \frac{Lmax_\lambda - Lmin_\lambda}{QCALmax - QCALmin} \right\} \times (DN - Q_{CALmin}) + Lmin_\lambda$$

$$\rho_e = (\pi \times L_\lambda \times d^2) / (E_{SUN\lambda} \times \cos\Theta_r)$$

$$\rho = \frac{\pi \times (L_\lambda - L_p) \times d^2}{T_v \times [(E_{SUNN\lambda} \times \cos\Theta_s \times T_z) + E_{down}]}$$

L_λ value as radiance,

DN'Q_{CAL} cell value digital number,

$L_{MIN\lambda}$ spectral radiance scales to Q_{CALMIN},

$L_{MAX\lambda}$ spectral radiance scales to Q_{CALMAX},

Q_{CALMIN} minimum quantized calibrated pixel value,

Q_{CALMAX} maximum quantized calibrated pixel value,

$\rho\lambda$ Unit-less plantary reflectance,

d Earth-Sun distance in astronomical units,

$E_{SUN\lambda}$ mean solar exoatmospheric irradiances,

θs solar zenith angle,

T_V atmospheric transmittance in the viewing direction,

T_Z atmospheric transmittance in the illumination direction,

$$L_{\lambda Pixel,Band} = \frac{K_{Band} \times q_{Pixel,Band}}{\Delta \lambda_{Band}}$$

$$L_P = L_{(\lambda Pixel,Band)min} - \frac{0.01 \times (ESUN_\lambda \times \cos\theta_s \times T_z) + E_{down}] \times T_v}{\pi \times d^2}$$

$L_{\lambda Pixel,Band}$ top-of-atmosphere spectral radiance image pixels [W-m-2-sr-1-μm-1],

K_{Band} absolute radiometric calibration factor [W-m-2-sr-1-count-1],

$q_{Pixel,Band}$ radiometrically corrected image pixels [counts] and

$\Delta \lambda_{Band}$ effective bandwidth [μm] for a given band

NDVI is one of most common vegetation indices for studying vegetation using the satellite images (Rouse *et al.,* 1973; Amiri *et al.,* 2010):

$$NDVI = \frac{NIR-RED}{NIR+RED}$$

2-Satellite image elements selection adopted for each site in field measurements: According to Hmeidan *et al.,* 2016 "in press" was adopted to symbolize field sites on satellite images.
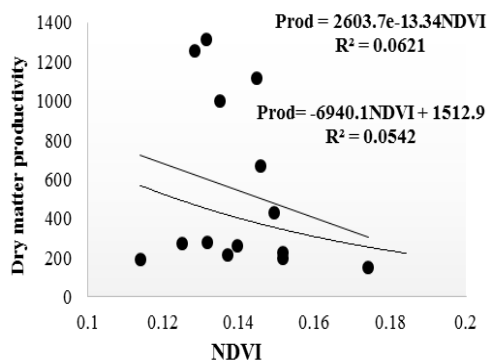
E_{down} down welling diffuse irradiance.

Then, BKA_{DN}, KVA_{DN} values were converted into GS values based on following equations:

$$\rho_{\lambda Pixel,Band} = \frac{L_{\lambda Pixel,Band} \times d_{ES}^2 \times \pi}{E_{sun\lambda Band} \times \cos(\theta_s)}$$

Results

1-NDVI analysis according to DN:

Fig. 2 shows the relationship between PDMP and NDVI calculated according to DN values. All functions of correlation relationship were weak and insignificant at 5% and 1% levels. Correlation coefficient exceeds 0.06 for exponential relationship despite of that relationship shown which decreased in PDMP as value of NDVI increased.

2-NDVI analysis according to TOA:

Fig. 3 shows the correlation between PDMP and NDVI calculated according to TOA values. All functions of the correlation relationship were relatively good and significant at 5% and 1%. In the same figure, value of PDMP is generally increased with increasing of NDVI. NDVI values ranged between 0.075 and 0.105 for all field sites.
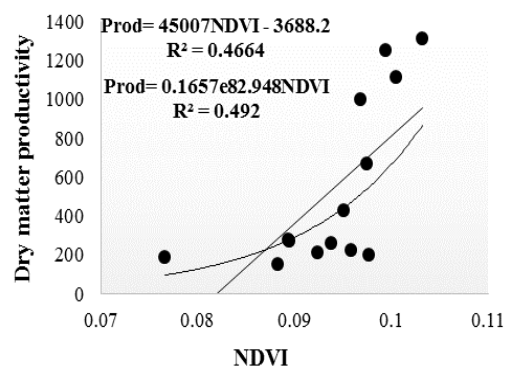

Fig. 2. Prod, NDVI relationship in DN

Fig. 3. Prod, NDVI relationship in TOA

3-NDVI analysis according to GS: Fig. 4 shows the correlation between plant dry matter productivity and NDVI calculated according to GS after the correction of atmospheric errors with a significant relationship at 5% and 1% levels. Correlation coefficient was 0.78 for exponential relationship and 0.73 for linear relationship.
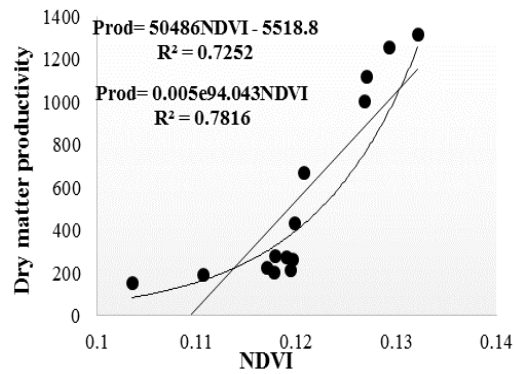
Fig. 4. Prod, NDVI relationship in GS

4-Relationship extraction between L8$_{NDVI}$ and BKA$_{NDVI}$, KVA$_{NDVI}$: a relationship was established between each of Time-compliant satellite images and differences in spatial resolution. Relationships were presented in Table 2.

Table. 2. Relationship between L8NDVI and BKANDVI, KVANDVI

R²	Relationship		Date	Image
0.66**	NDVI$_{L8}$ = 1.0851 NDVI$_{KVA}$ + 0.165	**DN**	2015/04/18	**KVA**
0.52**	NDVI$_{L8}$ = 0.3605 NDVI$_{KVA}$ + 0.082	**TOA**	2015/04/14	**L8**
0.74 **	NDVI$_{L8}$ = 1.3865×NDVI$_{KVA}$ - 0.1238	**GS**		
0.44**	NDVI$_{L8}$ = 0.0905 NDVI$_{KVA}$ + 0.0814	**DN**	2015/04/23	**KVA**
0.53**	NDVI$_{L8}$ = 0.3319 NDVI$_{KVA}$ + 0.0806	**TOA**		
0.74 **	NDVI$_{L8}$ = 0.8336×NDVI$_{KVA}$- 0.0128	**GS**	2015/04/30	**L8**
0.71**	NDVI$_{L8}$ = 0.5437 NDVI$_{BKA}$ + 0.0414	**DN**	2015/07/30	**BKA**
0.61**	NDVI$_{L8}$ = 0.7521 NDVI$_{BKA}$ + 0.0724	**TOA**		
0.88 **	NDVI$_{L8}$ = 0.8541×NDVI$_{BKA}$ -0.0299	**GS**	2015/08/04	**L8**
0.57**	NDVI$_{L8}$ = 0.6615 NDVI$_{BKA}$ + 0.0231	**DN**	2014/10/09	**BKA**
0.71**	NDVI$_{L8}$ = 0.5751 NDVI$_{BKA}$ + 0.0834	**TOA**	2014/10/04	**L8**
0.86 **	NDVI$_{L8}$ = 1.7493×NDVI$_{BKA}$ - 0.1169	**GS**		

Then, a relationship was compensated between L8$_{NDVI}$ in terms of BKA$_{NDVI}$, KVA$_{NDVI}$ (for each date of corresponding dates of images) in relationships described in PDMP calculation from L8 images in terms of NDVI according to TOA and GS values (Both exponential and linear) to estimate plant PDMP from BKA and KVA images for each previous case.

5-NDVI analysis to PDMP determination: NDVI values and its variations were analyzed according to correlations relationship derived for each case; then, PDMP was estimated to be predicted during studied months based on

NDVI value of satellite images according to L8 images relations and relationships in Table 2 for other images. During spring and beginning of summer (grazing season in the desert) for available images in 2015 and 2014, objective maps for study area concerning PDMP were proposed.

5-1-According to DN values: despite of relatively strong correlation between two types of satellite images used in case of using DN to calculate NDVI, the correlation between PDMP and NDVI is weak and insignificant at levels of 5% and 1%, and PDMP values showed a narrow range (100-250 kg/h) for the same

NDVI values which ranged from 0.11 to 0.175. In the same context, PDMP values varied from 200 to 1300 kg/h within NDVI (0.13-0.15). Relationships (exponential and linear) showed that PDMP decreased with the increase of NDVI. Therefore, there is no benefit in estimating PDMP according to DN values because it does not represent the reality.

5-2-According TOA and GS

5-2-1-NDVI and PDMP analysis for mid-April 2015: KVA$_{PDMP}$ average values on 18/04/2015 were 15 kg/h level when calculated according to TOA (Fig.5B). Values varied between 0-33 kg/h for the study area. KVA$_{PDMP}$ average according to GS was 42 kg/h and values ranged between 0-90 kg/h for the study area as shown in Fig.5A. Then, objective maps were produced for the area (Figs. 5C&D).
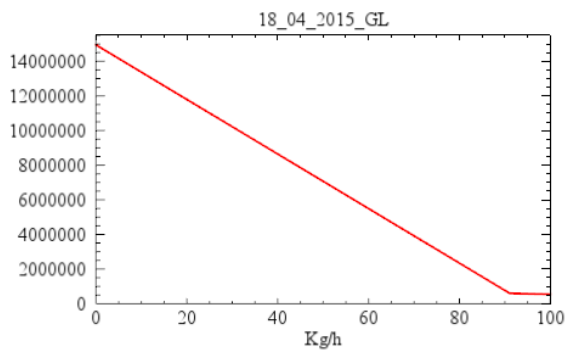
Fig. 5A. **KVA$_{PDMP}$ 18/04/2015 GS**
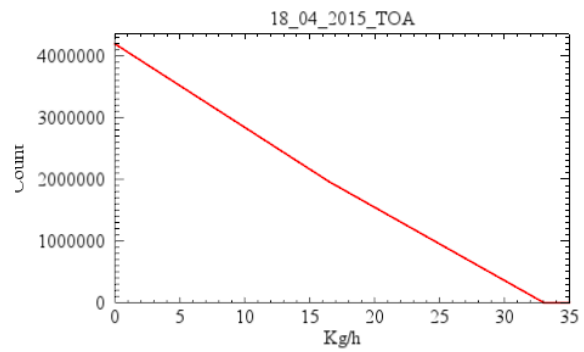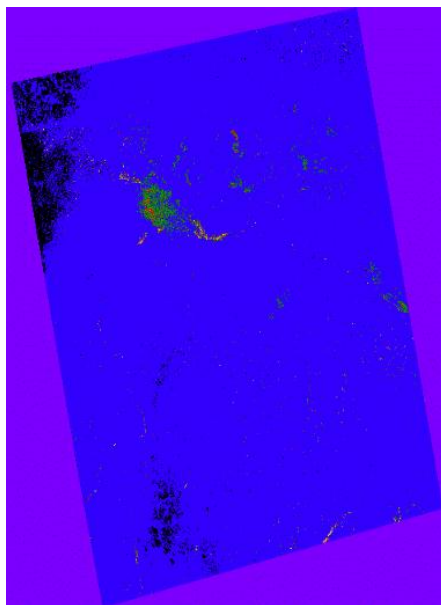

Fig. 5B. **KVA$_{PDMP}$ 18/04/2015 TOA**

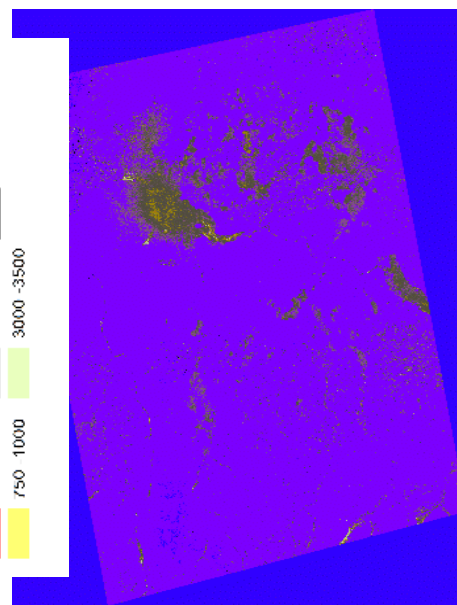**Fig. 5C.** KVA$_{PDMP}$ map 18/04/2015GS

Fig. 5D. KVA$_{PDMP}$ map 18/04/2015TOA

5-2-2-NDVI and PDMP analyses for end - April 2015: KVA$_{PDMP}$ average values on 23/04/2015 were 969 kg/h level when calculated according to TOA (Fig.6B). Values varied between 1200-2000 kg/h for the whole study area.

KVA$_{PDMP}$ average according to GS was 214 kg/h and values ranged between 50-450 kg/h for the study area as shown in Fig.6.A. Then, objective maps were produced for the area (Figs. 6C&D).
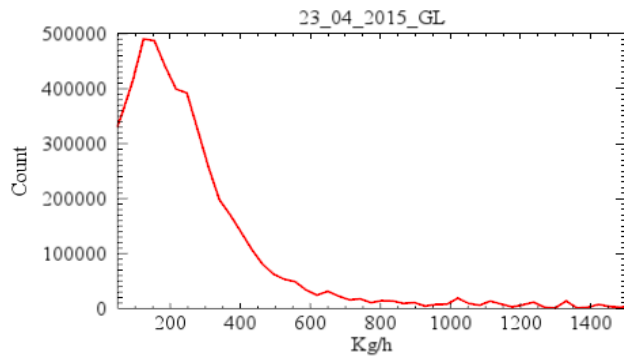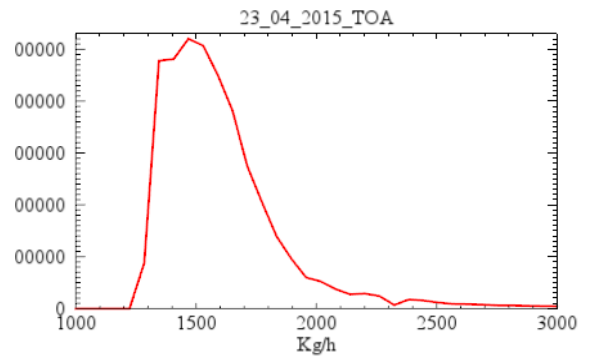
Fig. 6A. KVA_PDMP 23/04/2015 GS

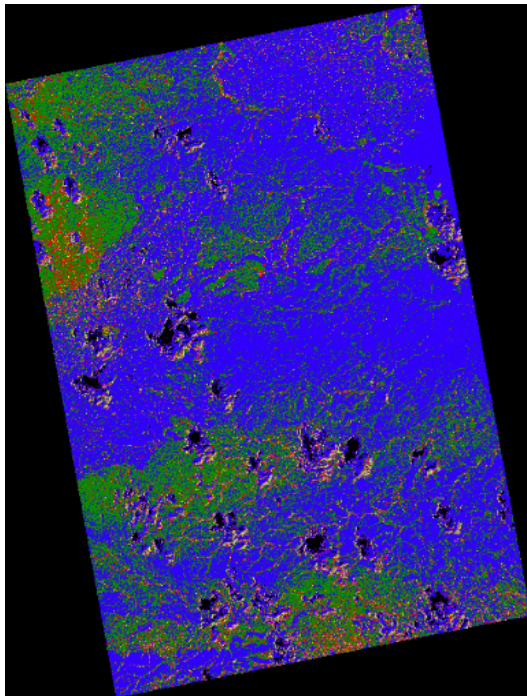
Fig. 6B. KVA_PDMP 23/04/2015 TOA

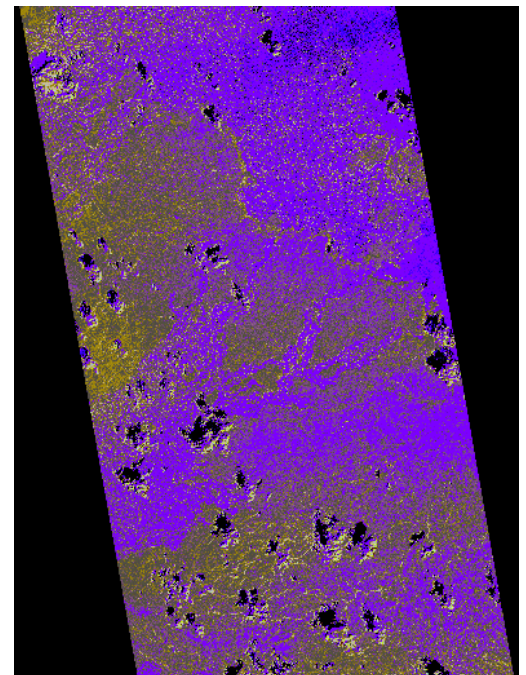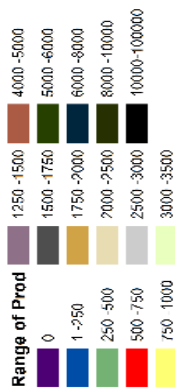**Fig. 6C.** KVA_PDMP map 23/04/2015GS

Fig. 6D. KVA_PDMP map 23/04/2015 TOA

5-2-3-NDVI and PDMP Analysis for August 2015: BKA_PDMP average values on 30/07/2015 were 3254 kg/h level when calculated according to TOA (Fig.7.B). Values varied between 3000-4500 kg/h for the study area. BKA_PDMP average according to GS was 22 kg/h and values ranged between 0-60 kg/h for the study area as shown in Fig.7A. Then, objective maps were produced for the area (Figs.7C&D)**.**
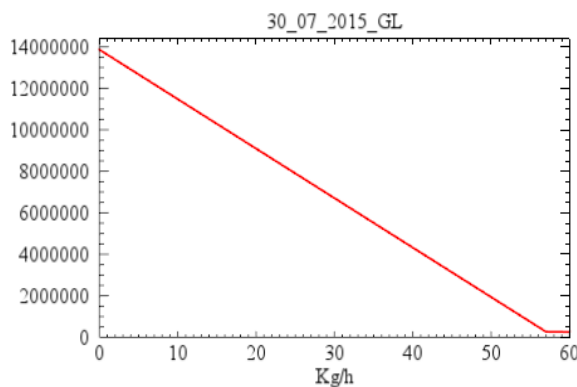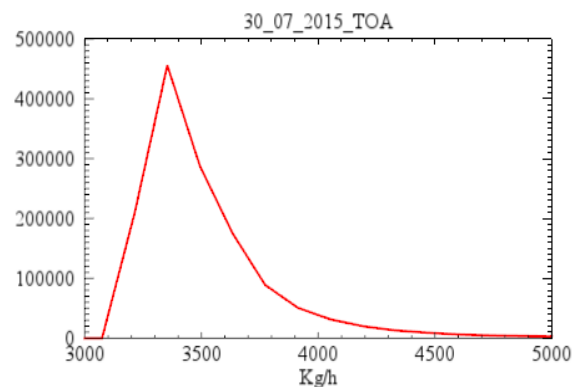

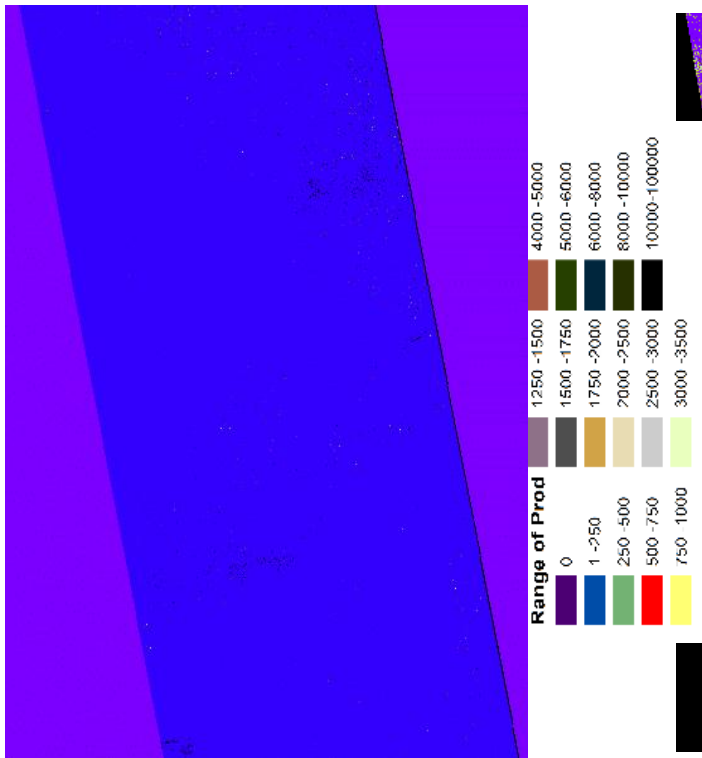**Fig. 7A.** BKAPDMP 30/07/2015 GS

Fig. 7B. BKAPDMP30/07/2015 TOA

Fig. 7C. BKA$_{PDMP}$ map 30/07/2015 GS
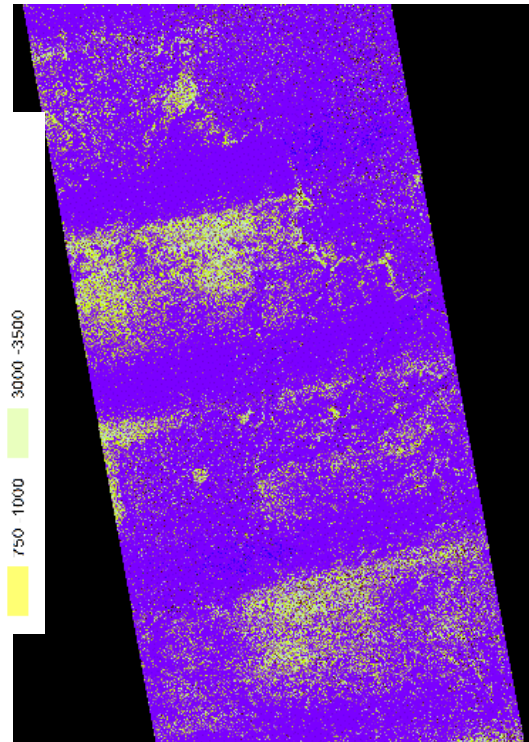
Fig. 7D. BKA$_{PDMP}$ map 30/07/2015 TOA

5-2-4-NDVI and PDMP analyses for October 2014: BKA$_{PDMP}$ average values on 09/10/2014 were 576 kg/h level when calculated according to TOA (Fig.8B). Values varied between 0-100 kg/h for the study area. BKA$_{PDMP}$ average according

to GS was 563 kg/h and values ranged between 0-150 kg/h for the study area as shown in Fig.8A. Objective maps were produced for area (Figs.8.C&D).

Fig. 8A. BKA$_{PDMP}$ 09/10/2014 GS

Fig. 8B. BKA$_{PDMP}$ 09/10/2014 TOA

Fig. 8C. BKA_PDMP map 09/10/2014 GS

Fig. 8D. BKA_PDMP map 09/10/2014TOA

Discussion

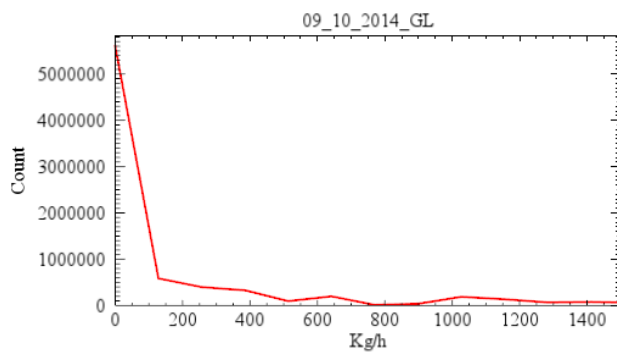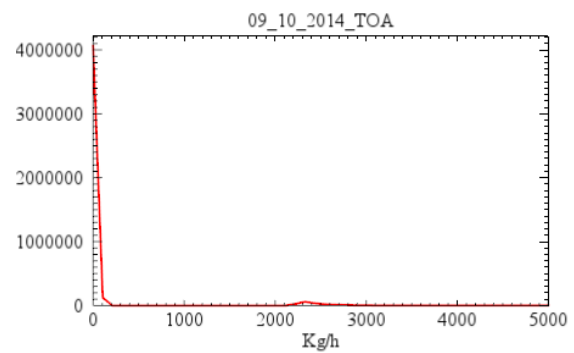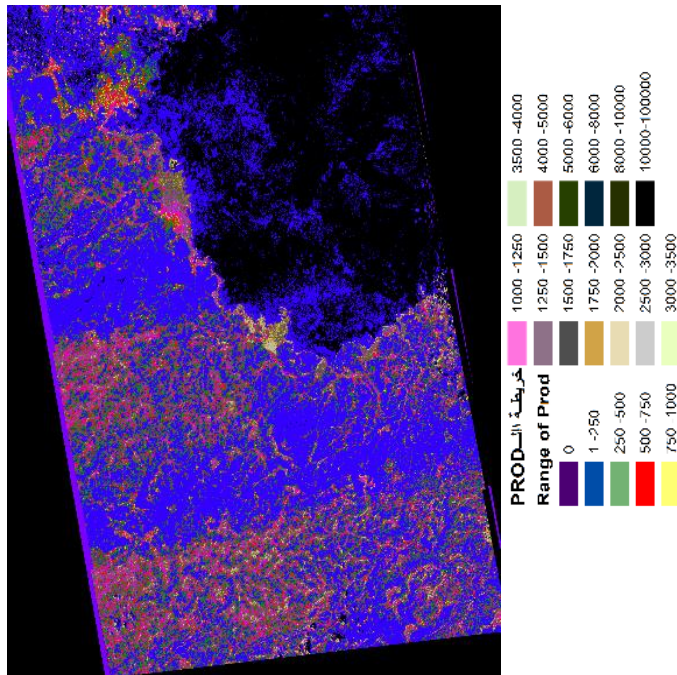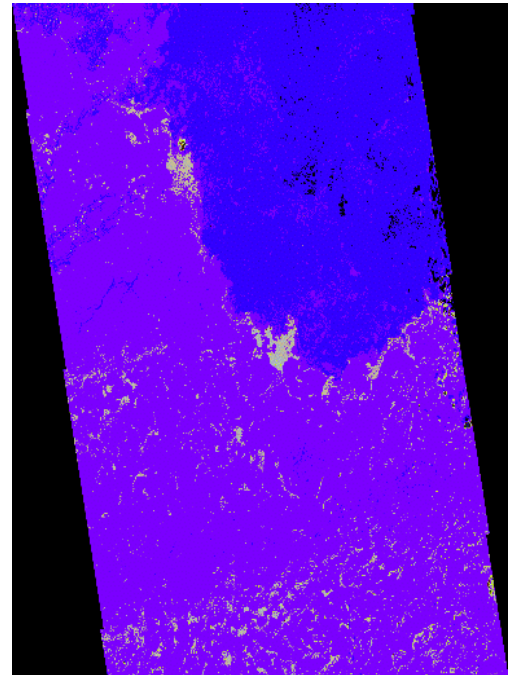Results showed that the use of satellite images in DN form for estimating al-Sweeda Badia rangeland productivity is not good because NDVI values derived from previous images according to DN values are flawed due to several factors especially caused by atmosphere that caused geometrical distortions on reflected radiation from targets, which had a significant impact on previous values and led to the increased NDVI accompanied by the decreased PDMP; this is a big mistake.

Converting DN values into TOA values led to the sensitivity increase to relatively better PDMP estimate in spite of estimated PDMP values in some locations that are relatively high for some images used. But the use of TOA values was not good in all images because it gave false results as what happened in August 2015, where satellite images according to these values gave very high PDMP results, which was reversing field validation.

But when GS values were used after atmospheric errors correction, it increased the ability of satellite images in this formula to estimate PDMP, and gave a good indication and situation of studied rangeland reality away from any factors affecting the values; a high quality use was shown by PDMP estimated in June 2015 through field validation, and August of the same year.

Conclusions

Satellite images and specialized software can be used to estimate rangeland productivity, where raw satellite images in DN values contain geometrical distortions caused by terrain, climate, changes in velocity of sensor and its elevation in addition to radiation refraction in atmosphere. To overcome these errors, GS values were extracted after atmospheric errors were corrected. Thus, rangelands state and PDMP estimation can be predicted through NDVI calculation of recent satellite images for the same study area based on GS values without field measurements requiring time and effort.

However, studied results can only be generalized after studying much number of modern BKA, and KVA satellite images to make statistical reliability for these results.

Recommendations

It is recommended to use BKA, and KVA satellite images according to GS values after atmospheric errors correction in case of studying rangelands, and productivity changes. And DN or TOA are not proposed to apply because satellite images in those cases have geometric distortions that affect values and do not produce accurate results.

References

Abuzar, M.; K, Sheffield; D, Whitfield; M, O'Connell and A, McAllister. 2014. Comparing inter-sensor NDVI for the analysis of horticulture crops in south-eastern Australia. American Journal of Remote Sensing; 2(1): 1-9.

Al-Khalif, H; N. Daoud; H. Shehab. 2009. Evaluation of the effectiveness of cultivation methods of pastoral plants in palmyra badia. Master Thesis, Department of Environmental Forestry, Faculty of Agriculture, Damascus University, Syria.

Amiri, F., B. Abdul Rashid and M. Shariff. 2010. Using remote sensing data for vegetation cover assessment in semi-arid rangeland of center province of Iran. In World Applied Sciences Journal, 11 (12): 1537-1546, ISSN 1818-4952.

Chander, G & B. Markham. 2003. Revised landsat5 TM radiometric calibration p rocedures and post calibration dynamic ranges geosciences and remote sensing. IEEE Transactions on, 41: 2674-2677.

Chander, G., B. L. Markham and D. L. Helder. 2009. Summary of current radiometric calibration coefficients for Landsat MSS, TM, ETM+, and EO-1 ALI sensors. Remote Sens. Environ. 2009: 113, 893–903.

Deep. R; Idris, Y., 2006. Using ASTER satellite images in rangeland studying. Diploma Thesis. Department of Geography, University of Damascus, Syria.

Diop, C., 1998. Measurements required in rangeland monitoring. Lecture presented in: Training course on management, improvement and monitoring of rangeland "Directorate of Badia and Sheep, Ministry of Agriculture, Damascus, Syria.

Eremeev.V; V. Ermakov; A. Kuznetcov; O. Nikonov; V. Pobaruev and V. Poshekhonov. 2014. Ground pressing technologies of "CANOPUS-V" and "BKA" information. Proc. SPIE 9241, Sensors, Systems, and Next-Generation Satellites XVIII, 92411V; doi:10.1117/12.2066629

Felde, G. W., G. P. Anderson, S. M. Adler-Golden, M. W. Matthew, and A. Berk, 2003. Analysis of hyperion data with the FLAASH atmospheric correction algorithm. Algorithms and Technologies for Multispectral, Hyperspectral, and Ultraspectral Imagery IX" SPIE Aerosense Conference, Orlando. 21-25 April: 90-92.

Fwal, A., S. Eid, M. Rokaya. 2009. Using remote sensing techniques and geographical information system in estimating rangeland capacity for selected areas of Rakka Badia. PhD Thesis Department of Geography, University of Damascus, Syria.

Hanqiu, X and T. Zhang. 2011. Comparison of landsat-7 ETM+ and ASTER NDVI measurements. Remote Sensing of the Environment: The 17th China Conference on Remote Sensing; Proc. of SPIE vol. 8203 82030K-1. Proc. SPIE 8203, Remote Sensing of the Environment: doi: 10.1117/12.910397.

Hmeidan, G., A. Alboody; S. Moussa; N. Daoud; A. Yaghi; E.Alkhaled. 2016. Analysis of NDVI changes and using NDVI to estimate plant productivity of dry matter for an area of Sweda Badia by reflectance-at-ground level for landSat 7&8 satellite images. The Arab Journal for Arid Environments. (In press)

Liqin ,C; T, LIU and L, Wei. 2014. A comparison of multi-resource remote sensing data for vegetation indices. IOP Conf. Ser.: Earth Environ. Sci. 17, 012067 doi:10.1088/1755-1315/17/1/012067.

Mishra , N; M. O. Haque, L. Leigh , A. David , H. Dennis and B. Markham. 2014. Radiometric cross calibration of landsat 8 operational land imager (OLI) and Landsat 7 enhanced thematic mapper plus (ETM+). Remote Sens., 6: 12619-12638.

Miura, T; H, Yoshioka; K, Fujiwara and H, Yamamoto. 2008. Inter-comparison of ASTER and MODIS surface reflectance and vegetation index products for synergistic applications to natural resource monitoring. Sensors, 8, 2480-2499.

Nekrasova, V and E. Makushevaa. 2012. Satellite CANOPUS-V' images Processing technology development for cartography purposes based on prelaunch simulation. International Archives of the Photogrammetry, Remote Sensing and Spatial Information Sciences, Volume XXXIX-B4, 2012 XXII ISPRS Congress, Melbourne, Australia.

Nordblom, T. L, A. V.Goddchild, F. Shomo, and G. Gintzburger. 1997. Dynamics of feed resources in mixed farming systems of

West/Central Asia-North Africa. In C. Renard (Ed.), Crop residues in sustainable mixed crops/livestock farming systems (pp. 131–147). Wallingfold (UK): CAB International.

Owensby, C.E. 1973. Technical notes: modified step-point system for botanical composition and basal cover estimates. Journal of Range Manage. 26:302-303

Parente,C., 2013. TOA reflectance and NDVI calculation for Landsat 7 ETM+ images of Sicily. Electronic International Interdisciplinary Conference, SECTION11. Ecology, Forestry, Earth Science.

Roland. G., and M. Ilaiwib. 2004. Assessment of rangeland degradation and development of a strategy for rehabilitation. Remote Sensing of Environment, 90: 490 – 504.

Ronald B. S., 2005. Computing radiances, reflectance and albedo from DN's". Report. http:// www.yale.edu/ceo/Documentation /Computing Reflectance from DN. Downloaded at 10/05/2013.

Rouse, J. W., R. H. Haas, J. A. Schell, and D. W. Deering. 1973. Monitoring vegetation systems in the Great plains with ERTS", Third ERTS Symposium, NASA SP-351 I: 309- 317.

Soudani, K; C, François; G, Maire; V, Dantec and E, Dufrêne. 2006. Comparative analysis of IKONOS, SPOT, and ETM+ data for leaf area index estimation in temperate coniferous and deciduous forest stands. Remote Sensing of Environment Vol:102, Issues 1–2, 30, P:161–175.

Tanser, F. C and A. R. Palmer. 1999. The application of a remotely-sensed diversity index to monitor degradation patterns in a semi-arid, heterogeneous, South African landscape. Journal of Arid Environments, 43: 477– 484.

The Arab Center for the Studies of Arid Zones and Dry Lands, Syria (ACSAD). 2004. Report of natural resources survey project in Syrian Badia using remote sensing techniques and geographical information system. Prepared for the Ministry of Agriculture in Syrian Arab Republic.

Théau, J; Temuulen T and W, Keith. 2010. Multi-sensor analyses of vegetation indices in a semi-arid environment. GIScience & Remote Sensing, 47, No. 2, p. 1–XXX. DOI: 10.2747/1548-1603.47.2.1

Thenkabail, P. S., 2004. Inter-sensor relationships between IKONOS and Landsat-7 ETM+ NDVI data in three ecoregions of Africa. International Journal of Remote Sensing Vol:25, P:389-408.

Yin, H; T, Udelhoven; R, Fensholt; D, Pflugmacher and P, Hostert. 2012. How normalized difference vegetation index (NDVI) trends from advanced very high resolution radiometer (AVHRR) and systeme probatoired 'Observation de la Terre VEGETATION (SPOT VGT) time series differ in agricultural areas: An inner Mongolian case study. Remote Sens., 4, 3364-3389; doi:10.3390/rs4113364.

برآورد حاصلخیزی ماده خشک گیاهان در مراتع السویدا بادیا کشور سوریه با استفاده از تصاویر ماهواره‌ای BKA و KVA

غدیر همیدان^{الف}، احد البودی^ب

^{الف}گروه دریافت و تصحیح تصاویر، مرکز تکنولوژی فضایی، سازمان عمومی سنجش از دور، دمشق، سوریه *(نگارنده مسئول)، پست الکترونیک: ghadir.hmeidan@yahoo.com

^برئیس گروه تلفیق و آزمایش مرکز تکنولوژی فضایی، سازمان عمومی سنجش از دور، دمشق، سوریه

چکیده. برآورد ماده خشک گیاهی برای مدیریت مراتع با دقت بالا جهت مدیران بسیار مهم است. هدف از تحقیق حاضر مقایسه دقت برآورد ماده خشک گیاهی با استفاده از شاخص پوشش گیاهی (NDVI) بدست آمده از تصاویر ماهواره BKA و KVA با در نظر داشتن روشهای مختلف پردازش تصاویر ماهواره‌ای برای منطقه السویدا کشور سوریه در طی ماه‌های فروردین، اردیبهشت، خرداد و تیر سال ۱۳۹۴ و مهر ماه سال ۱۳۹۳ بود. شاخص گیاهی NDVI با توجه به ارزش شماره رقم و ارزشهای جوی حساب شد و سپس پوشش سطح زمین بعد از تصحیح اتمسفری از روی شبیه‌سازی تصاویر ماهواره لندست ۸ اندازه‌گیری شده از سطح زمین محاسبه شد. بین تصاویر دو سری زمانی ماهواره رابطه‌ای برقرار گردید. سپس این روابط توسط ماده خشک گیاهی ماهوراه لندست ۸ سازگار شدند. متوسط تولید ماده خشک با توجه به شرایط سطح زمین و تصاویر ماهواره به ترتیب برای تاریخهای مورد نظر یعنی فروردین به میزان ۱۵ الی ۴۲، اردیبهشت ۲۱۴ الی ۹۶۹، خرداد ۳۲۵ و تیر ۴۲۲ در سال ۱۳۹۴ و در مهرماه سال ۱۳۹۳ بین ۵۶۳ و ۵۷۶ کیلوگرم در هتار بودند. رابطه همبستگی ضعیف غیر معنی داری بین ارزش شماره رقم (DN) و ماده خشک به میزان کمتر از ۶۳ درصد بود. این این رابطه همبستگی برای سطوح مختلف بالای اتمسفر نیز ضعیف و اما معنی‌دار به میزان کمتر از ۵۰ درصد بود. بعد از پردازش تصویر و انجام تصحیحات اتمسفری بر روی تصاویر روابط همبستگی قوی شدند و به میزان بیش از ۷۰ درصد رسیدند که در نتیجه آن در سطح یک و پنج درصد معنی‌دار شدند و با اندازه‌گیری‌های میدانی در سال ۱۳۹۳ همخوانی داشتند. همچنین با استفاده از تصاویر جدید بین شاخص پوشش گیاهی NDVI و ماده خشک گیاهی رابطه برقرار شد. این روابط بدست آمده برای برآورد ماده خشک گیاهی بکار رفتند و سپس نقشه‌های خروجی به شکل وکتور تولید شدند. نتایج نشان داد که شماره رقم (DN) تصاویر ماهواره‌ای همانند ارزش‌های عامل بالای اتمسفر بودند اما در مقدار کمتر که تحت تاثیر تغییرات سه بعدی و آب و هوا و نیز انعکاس اشعه در فضای اتمسفر قرار داشتند. نیز باید گفت که بکار بردن پوشش سطح زمین بعد از انجام تصحیحات اتمسفریک بر روی تصاوی در مراتع برای پیش‌بینی و برآورد میزان ماده خشک گیاهی خوب بود.

کلمات کلیدی: حاصلخیزی ماده خشک گیاهی، NDVI، ماهواره لندست ۸، شماره دجیتال، بالای اتمسفر، سطح زمین، سطوح مختلف تصحیح تصاویر ماهواره‌ای